Biochemical and Biophysical Research Communications 463 (2015) 268–274

Contents lists available at ScienceDirect

Biochemical and Biophysical Research Communications

journal homepage: www.elsevier.com/locate/ybbrc

DNA damage, lysosomal degradation and Bcl-xL deamidation in doxycycline- and minocycline-induced cell death in the K562 leukemic cell line

Mona Fares [a], Manuchehr Abedi-Valugerdi [a], Moustapha Hassan [a, b], Zuzana Potácová [a, *]

[a] Experimental Cancer Medicine (ECM), Clinical Research Center (KFC), Novum, Department of Laboratory Medicine, Karolinska Institutet, Stockholm, Sweden

[b] Clinical Research Center (KFC), Novum, Karolinska University Hospital Huddinge, Stockholm, Sweden

ARTICLE INFO

Article history:
Received 22 April 2015
Available online 27 May 2015

Keywords:
Cell death
K562 cell line
Doxycycline
Minocycline
Apoptosis

ABSTRACT

We investigated mechanisms of cytotoxicity induced by doxycycline (doxy) and minocycline (mino) in the chronic myeloid leukemia K562 cell line. Doxy and mino induced cell death in exposure-dependent manner. While annexin V/propidium iodide staining was consistent with apoptosis, the morphological changes in Giemsa staining were more equivocal. A pancaspase inhibitor Z-VAD-FMK partially reverted cell death morphology, but concurrently completely prevented PARP cleavage. Mitochondrial involvement was detected as dissipation of mitochondrial membrane potential and cytochrome C release. DNA double strand breaks detected with γH2AX antibody and caspase-2 activation were found early after the treatment start, but caspase-3 activation was a late event. Decrement of Bcl-xL protein levels and electrophoretic shift of Bcl-xL molecule were induced by both drugs. Phosphorylation of Bcl-xL at serine 62 was ruled out. Similarly, Bcr/Abl tyrosine kinase levels were decreased. Lysosomal inhibitor chloroquine restored Bcl-xL and Bcr/Abl protein levels and inhibited caspase-3 activation. Thus, the cytotoxicity of doxy and mino in K562 cells is mediated by DNA damage, Bcl-xL deamidation and lysosomal degradation with activation of mitochondrial pathway of apoptosis.

1. Introduction

Inhibition of cell death can contribute to the resistance of leukemic cells to chemotherapy [1]. Cell death may be divided into distinct entities based on the morphological and biochemical features [2]. Apoptosis may be processed through an extrinsic or intrinsic pathway. The extrinsic pathway is initiated by extracellular stressors and propagated by the trans-membrane receptors in a caspase-dependent manner. The intrinsic apoptosis is a response to intracellular stress such as DNA damage or oxidative stress and is mediated by the mitochondrial outer membrane permeabilization (MOMP) in either the caspase-dependent or -independent pathway [2]. The loss of mitochondrial membrane potential ($\Delta\psi m$) with subsequent drop in ATP production is considered to be the point of no return along the apoptotic pathway [3]. Necrosis may be uncontrolled or programmed. The former is characterized by early loss of membrane integrity and dilation of organelles, the latter by receptor-interacting protein kinase (RIP)-1 and RIP-3 [4]. The lysosomes can contribute to any type of cell death [5].

Doxycycline (doxy) and minocycline (mino) are semi-synthetic derivatives of tetracyclines that exhibit anti-bacterial effects and antitumor activities in several cancer cell lines [6,7]. Doxy-induced apoptosis was associated with loss of $\Delta\psi m$, cytochrome C (cytC) release, Bcl-xL inhibition, caspase activation and intracellular ROS formation in colorectal and pancreatic cancer cell lines [6,7]. Mino-induced apoptosis was associated with caspase-3 activation and PARP-1 inhibition in ovarian cancer [8].

The leukemic K562 cell line established from a patient in blastic crisis of chronic myeloid leukemia (CML) possesses characteristics of CML [9] as cells express the p210 Bcr/Abl fusion protein and overexpress the antiapoptotic Bcl-xL protein [10]. The aim of our study was to assess the mechanisms of doxy- and mino-induced cytotoxicity in K562 cells.

* Corresponding author. Experimental Cancer Medicine (ECM), 6th floor, Clinical Research Center (KFC), Novum, Karolinska University Hospital Huddinge, 14186 Stockholm, Sweden.

E-mail addresses: mona.fares@ki.se (M. Fares), manuchehr.abedi-valugerdi@ki.se (M. Abedi-Valugerdi), moustapha.hassan@ki.se (M. Hassan), zuzana.potacova@ki.se (Z. Potácová).

http://dx.doi.org/10.1016/j.bbrc.2015.05.043

2. Materials and methods

2.1. Chemicals and reagents

Doxycycline hyclate, minocycline hydrochloride, chloroquine diphosphate, vinblastine sulfate and bongkrekic acid were purchased from Sigma Aldrich (Stockholm, Sweden); etoposide from Bristol-Myers Squibb (Bromma, Sweden); resazurin from R&D systems Inc. (Minneapolis, MN, USA); Z-VAD-FMK from Bachem AG (Bubendorf, Switzerland); cOmplete mini protease inhibitor cocktail from Roche AB (Stockholm, Sweden); RPMI 1640 media, Dulbecco's phosphate-buffer saline (PBS) and fetal bovine serum (FBS) from Invitrogen AB, (Stockholm Sweden).

2.2. Cell culture

The human myeloid HL-60 and lymphoblastic Jurkat cell lines were purchased from DSMZ (Braunschweig, Germany), the chronic myeloid K562 cell line from ATCC (LGC Promochem Ab, Borås, Sweden). Cells were seeded at concentrations of 2×10^5 cells/ml and cultured in RPMI 1640 medium supplemented with 10% heat-inactivated FBS (complete medium) at 37 °C in 95% humidified 5% CO_2 atmosphere. All experiments were performed in exponentially growing cells.

2.3. Treatment

Cells were treated with drugs in final concentrations of 0.5–500 μg/ml in complete medium. Cells treated in 0.02% dH_2O served as controls for solvent toxicity. Cells treated with etoposide (6 or 40 μg/ml) or vinblastine (Vb; 10 or 50 μg/ml) served as positive controls for cell death. Cells incubated in complete media served as controls.

Cells were treated with pan-caspase inhibitor Z-VAD-FMK in a concentration of 100 μM for 1 h. Then doxy or mino were added in a final concentration of 50 μg/ml and cells were incubated for 6, 24 and 48 h. Fresh Z-VAD-FMK was added to the cultures every 24 h.

Cells were incubated with the adenine nucleotide (ADP/ATP) translocator (ANT) inhibitor bongkrekic acid (BKA) in a final concentration of 100 μM for 4 h and then treated concomitantly with BKA (50 μM) and doxy or mino (50 μg/ml) for 48 h.

Cells were treated with the lysosomal inhibitor chloroquine (CQ) in final concentrations of 25 or 50 μM for 1 h followed by treatment with doxy or mino in concentrations of 50 μg/ml for 48 h.

2.4. Cell viability assay

Ten thousands cells per well were seeded in triplicate on 96 wells black microplates and incubated with doxy or mino (0.5–500 μg/ml) for 24 h. Then resazurin was added in a final concentration of 10% and cells were further incubated for 2 h at 37 °C. Fluorescence was read using FLUOstar Optima (BMG Labtech GmbH, Offenburg, Germany) at a wavelength of 590 nm. Viability of treated cells was expressed as a percentage of the viability of controls. The 50% inhibitory concentration (IC_{50}) was calculated as the drug concentration inducing 50% reduction in cell viability using GraphPad Prism 6 (GraphPad Software, Inc., La Jolla, CA, USA).

2.5. Assessment of cell death

100,000 cells were stained with annexin V (Becton Dickinson (BD), San Jose, CA, USA) in a concentration of 125 ng/ml and propidium iodide (PI) (Sigma Aldrich, Stockholm, Sweden) in a concentration of 5 μg/ml in 100 μl of annexin V binding buffer for 15 min at room temperature (RT) in the dark. Samples were analyzed using FACScan flow cytometer, CELL Quest software (BD) and free Flowing Software ver. 2.5.1 (created by Perttu Terho, Cell Imaging Core, Turku Centre for Biotechnology, Finland, http://www.flowingsoftware.com/).

Cell death morphology consistent with apoptosis (condensed chromatin and fragmented nuclei) or necrosis (increased cell size and loss of cellular architecture) was assessed using May-Grünwald-Giemsa staining on cytospun slides and expressed as a percentage of a minimum of 400 cells counted per slide.

2.6. Assessment of mitochondrial membrane potential ($\Delta\psi m$)

Cells were incubated with the mitochondrial probe tetramethylrhodamine methyl ester (TMRM) (Molecular Probes, Carlsbad, CA, USA) in a final concentration of 25 nM in PBS for 30 min at 37 °C. After washing, cells were re-suspended in PBS and analyzed using flow cytometry.

2.7. Western blot (WB) analysis

Cells were lysed in Tris-NaCl buffer (50 mM Tris pH 7.4, 150 mM NaCl, 25 mM EDTA, 1 mM NaF, cOmplete mini protease inhibitor cocktail, 1 mM PMSF and 1% Triton × 100) on ice for 30 min, then centrifuged at 10,000 g for 10 min at 4 °C.

To assess poly (ADP-Ribose) polymerase (PARP), cells were incubated in PARP extraction buffer (62.5 mM Tris pH 6.8, 6 M urea, 2% SDS, 10% Glycerol and 0.001% bromophenol blue) for 15 min at RT, then for another 5 min at 95 °C.

For subcellular fractionation, the cells were incubated in digitonin cytosolic buffer (5 mM Tris–HCl pH 7.4, 5 mM succinic acid pH 6.3, 10 mM $MgCl_2.6H_2O$, 0.5 mM EDTA, 147.5 mM KCl, 5 mM KH_2PO_4 and 0.005% digitonin) for 30 min on ice and then centrifuged at 10,000 g for 10 min at 4 °C. The supernatant (cytosolic fraction) was collected and the pellet was re-suspended in PBS containing cOmplete mini protease inhibitor (pellet fraction).

Protein concentrations were assessed using Pierce® BCA or 660 nm® protein assay kits (Pierce, Rockford, IL, USA) according the manufacturer's recommendations.

For protein separation, equal volumes of samples and 2x Laemmli buffer supplemented with 5% 2-mercaptoethanol were boiled for 5 min at 95 °C. Protein samples (10 or 20 μg) were separated on 12 or 15% SDS-PAGE and transferred to a PVDF or to nitrocellulose membranes, whichever appropriate. The membranes were blocked in 5% non-fat dry milk solution for 2 h at RT and incubated overnight with primary antibodies (Supplementary Table 1) at 4 °C. Then the membranes were rinsed and incubated with secondary antibodies conjugated with peroxidase (Amersham Pharmacia Biotech AB, Uppsala, Sweden) or IRDye®800CW or IRDye®680CW (LI-COR, Lincoln, NE, USA) for 1 h at RT. The proteins were visualized using SuperSignal West Pico Chemiluminescent substrate (Pierce) or ODYSSEY imaging system (LI-COR). Actin was used as a marker of equal protein loading.

2.8. Assessment of intracellular reactive oxygen species (ROS)

The intracellular ROS levels were assessed using OxiSelect™ Intracellular ROS assay Kit with green fluorescence (Cell Biolabs, San Diego, CA, USA). Following the treatment with doxy or mino, cells were incubated with 100 μM of 2′-7′-dichlorodihydrofluorescin (DCFH-DA) in media for 1 h at 37 °C. Then the cells were washed in PBS and the DCF fluorescence measured using FLUOstar Optima at wavelengths 485/520 nm.

2.9. Statistical analysis

Experiments were performed three times independently and the results are expressed as a mean ± SD wherever appropriate.

3. Results and discussion

3.1. Effect of TCNAs on viability of leukemic cell lines

Incubation of the human leukemic cell lines with doxy and mino for 24 h reduced the cell viability with the IC_{50ies} presented in Table 1.

Antitumor effects of doxy and mino have been reported in several cancer cell lines with IC_{50ies} between 10 and 30 μg/ml [7,8,11], but no genotoxic or cytotoxic effects were observed in lymphocytes [12]. Tolemeo et al. reported IC_{50} of doxy in HL-60 cells to be 8 μg/ml [13]. In our study, IC_{50ies} of doxy and mino are in close agreement with the reported IC_{50ies}. The K562 cell line possesses the Bcr/Abl tyrosine kinase fusion protein and therefore has been selected for further experiments. For studies on cytotoxicity mechanisms, we selected drug concentrations up to 50 μg/ml to strengthen the cytotoxic effects. In the following sections, drug concentrations of 50 μg/ml are reported if not stated otherwise.

3.2. Cell death

Doxy and mino induced cell death in an exposure-dependent manner as detected with annexin V and PI positivity (Fig. 1). Increase of annexin V+ and annexin V+/PI+ cells was accompanied by a shift to smaller and more granular cells consistent with apoptosis. Morphological changes consistent with cell death were detectable at 6 h and 24 h of incubation with doxy and mino, respectively. However, morphology was equivocal and the type of cell death could not be determined using morphological criteria.

Surprisingly, lower concentrations of doxy and mino (10 and 20 μg/ml) did not increase cell death compared to controls until 48 h of incubation. Considering the determined IC_{50ies}, greater effect was expected from a concentration of 20 μg/ml. The difference may be explained by fundamental differences between the methods. Annexin V/PI assesses features of individual dying cells, while the resazurin assay determines the metabolism of total cell mass. Morphological staining corroborated the levels of the total cell death from Annexin V/PI assay (Supplementary Figure 1).

3.3. Caspase activation in TCNAs-induced cell death

Activation of caspase-2, -3, -8 and -9 was observed after treatment with both doxy and mino. The 12 kDa fragment of caspase-2 was detected at 6 h after start of treatment. Further incubation resulted in a reduction and at 48 h total disappearance of the 48 kDa procaspase bands in cells treated with doxy and mino in concentrations of 50 μg/ml (Fig. 2A). The early caspase-2 activation was confirmed by detecting the caspase-2 intermediate fragment of 32 kDa at 6 h after incubation start using another caspase-2 antibody (Fig. 2B). Furthermore, the caspase-2 active fragment of 18 kDa was detected in the cytosolic fraction of doxy treated cells at 6 and 24 h after the start of incubation (Fig. 2C). Caspase-2 functions as an initiator as well as effector caspase [14]. Caspase-2 is located in the nucleus, Golgi complex and soluble cytoplasm. It is activated in response to cellular stress, such as DNA damage or oxidative stress [15]. In our study, only minor increase in the ROS levels was found, but DNA double strand breaks were detected. Thus, most likely, caspase-2 was activated in response to DNA damage.

The 23 kDa fragment of caspase-8 was detected at 24 h of incubation with both drugs. The 19 kDa and 15 kDa fragments of caspase-3 and the 37 kDa fragment of caspase-9 were first detected in cells treated with doxy for 24 h and with mino for 48 h (Supplementary Figure 2). Altogether, the cell death induced by both drugs is caspase-mediated.

Table 1
IC_{50} of doxy and mino in the human leukemic cell lines.

	Doxy			Mino		
	IC_{50} (μg/ml)	95% CI	R^2	IC_{50} (μg/ml)	95% CI	R^2
HL60	9.2	8.79–9.66	0.995	9.9	8.61–11.29	0.974
Jurkat	13.8	12.34–15.43	0.979	24.7	21.69–28.08	0.972
K562	33.9	28.7–40.1	0.882	23.4	19.77–27.79	0.89

CI = confidence interval.

3.4. PARP-1 and Z-VAD-FMK in TCNAs-induced cell death

The 85 kDa fragment of PARP-1 was detected at 48 h after the incubation start with doxy and mino. Pretreatment with the pan-caspase inhibitor Z-VAD-FMK effectively prevented PARP-1 cleavage (Supplementary Figure 3A). Moreover, Z-VAD-FMK reduced the doxy- and mino-induced cell death morphology at 24 and 48 h after the start of incubation. Cells with apoptosis-like features decreased more than cells with necrotic features. A slight shift in cell appearance from apoptosis-like morphology towards cellular swelling was observed. This shift was most distinct in cells treated concomitantly with doxy and Z-VAD-FMK (Supplementary Figure 3B).

We assessed the effect of 25 or 50 μM necrostatin-1 on TCNAs induced cell death, but the total cell death was not affected by necrostatin-1. These results further indicated involvement of apoptotic mechanisms in TCNAs-induced cell death.

3.5. TCNAs effect on the mitochondria

Translocation of cytC to cytosol was observed at 6 h after incubation start with doxy and mino. The release of cytC was not associated with Bax or BID activation as the 16 kDa and 18 kDa fragments of Bax and BID were not observed before 48 and 24 h, respectively. Nevertheless, the role of BID in cytC release could not be completely ruled out since the BID has been reported to possess proapoptotic activity even without cleavage of the molecule [16].

Doxy- and mino-induced loss of $\Delta\psi m$ was first observed at 12 h of incubation and progressed in a concentration- and incubation time-dependent manner. The loss of $\Delta\psi m$ is a cardinal feature of the mitochondrial pathway of apoptosis and is potentiated by opening of the permeability transition pore (PTP) [17]. PTP spans through both the inner and the outer mitochondrial membranes. It consists of the adenine-nucleotide translocator (ANT) in the inner and a voltage-dependent anion channel (VDAC) in the outer mitochondrial membrane. Cyclophilin D is inside the mitochondria [18]. In our study, pre-incubation of K562 cells with the PTP inhibitor BKA did not reduce the loss of $\Delta\psi m$ induced by doxy or mino. This result indicates that either the loss of $\Delta\psi m$ wasn't dependent on the PTP opening or the loss of $\Delta\psi m$ relied on the VDAC opening without contribution of other components (ANT/cyD) [19]. The VDAC is considered to be the core component of the PTP. Bcl-xL and Bax interact with the VDAC channel and the Bax to Bcl-xL ratio controls the degree of the opening [20]. In our study, doxy and mino induced reduction of the Bcl-xL protein levels that might facilitate the Bax-VDAC interaction.

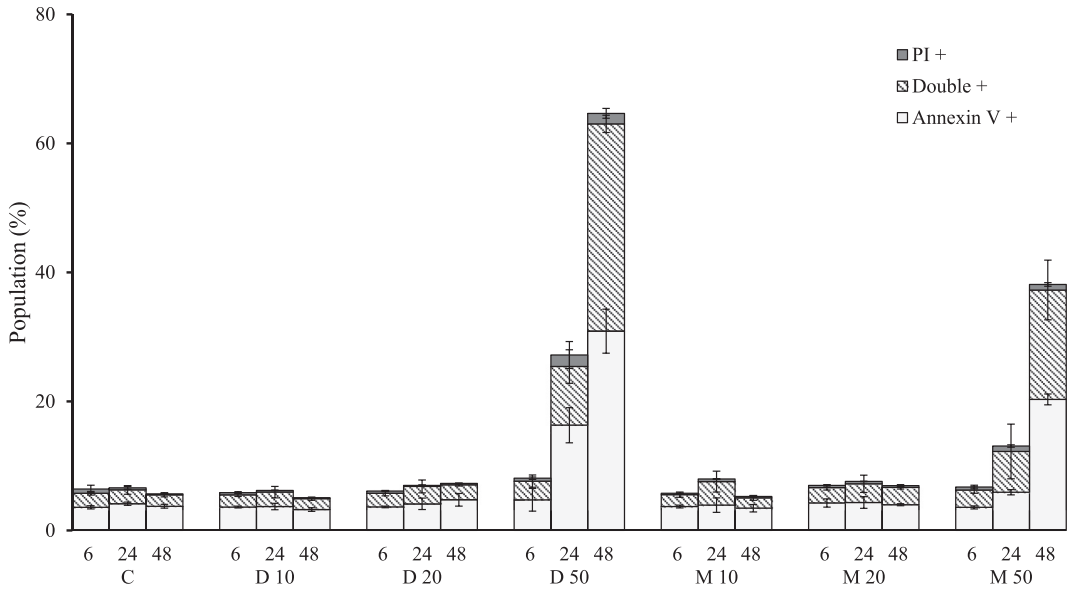

Fig. 1. *TCNAs-induced cytotoxicity in K562 cells*. Cells were incubated with doxy or mino (10, 20 and 50 μg/ml) for 6, 24 and 48 h. Cells were stained with annexin V/PI and analyzed using flow cytometry. Cell subpopulations were estimated as a percentage of 10,000 events. The results are expressed as mean ± SD of three independent experiments.

3.6. Expression and post-translational modification of the Bcl-xL and DNA damage

Doxy affected the expression of the Bcl-xL protein. The full-length 26 kDa protein band was reduced at 24 h and almost disappeared at 48 h after the incubation start. Mino-induced effect on the Bcl-xL protein level was similar, but less pronounced compared to doxy (Fig. 3A). We corroborated the finding by another Bcl-xL antibody (clone 54H6) (Fig. 3B). This antibody detects Bcl-xL as two bands, 32/33 kDa and 30 kDa, respectively. Besides the decrease of Bcl-xL protein levels, doxy and mino induced changes in the electrophoretic mobility of the Bcl-xL molecule. The expression of the 32/33 kDa band increased at 6 h of incubation with doxy and mino compared to the controls. At later time points, the levels of the Bcl-xL decreased in an incubation time-dependent manner (Fig. 3B).

The 32/33 kDa band was reported to be a result of the Bcl-xL phosphorylation or deamidation and was associated with loss of the antiapoptotic effect. The Bcl-xL molecule is predominantly phosphorylated on Serine 62, while phosphorylation on other sites is less likely [21]. The Bcl-xL molecule contains two labile asparaginyl sites at positions 52 and 66 which are prone to deamidation in response to cellular stress such as DNA damage or oxidative stress [22].

In order to identify the modification of the Bcl-xL molecule, we used etoposide as a control for deamidation and vinblastine as a control for Serine 62 phosphorylation. We could not demonstrate phosphorylation of Bcl-xL at Serine 62 using a specific antibody (p-

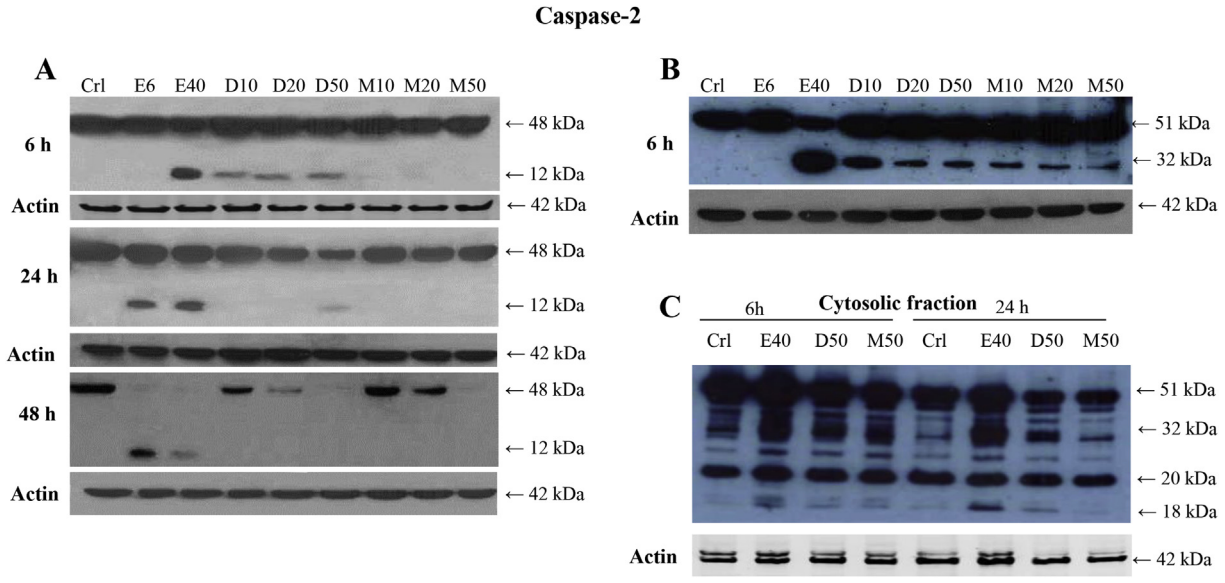

Fig. 2. *Caspase-2 activation in TCNAs treated cells*. Cells were incubated with doxy or mino (10, 20 and 50 μg/ml) for up to 48 h. Cells incubated with etoposide (6 and 40 μg/ml) served as positive controls, cells in complete medium as controls. Proteins were analyzed using Western blot. (A) Caspase-2 (C2). (B) Caspase-2 (11B4). (C) Caspase-2 (11B4) in cytosolic fraction.

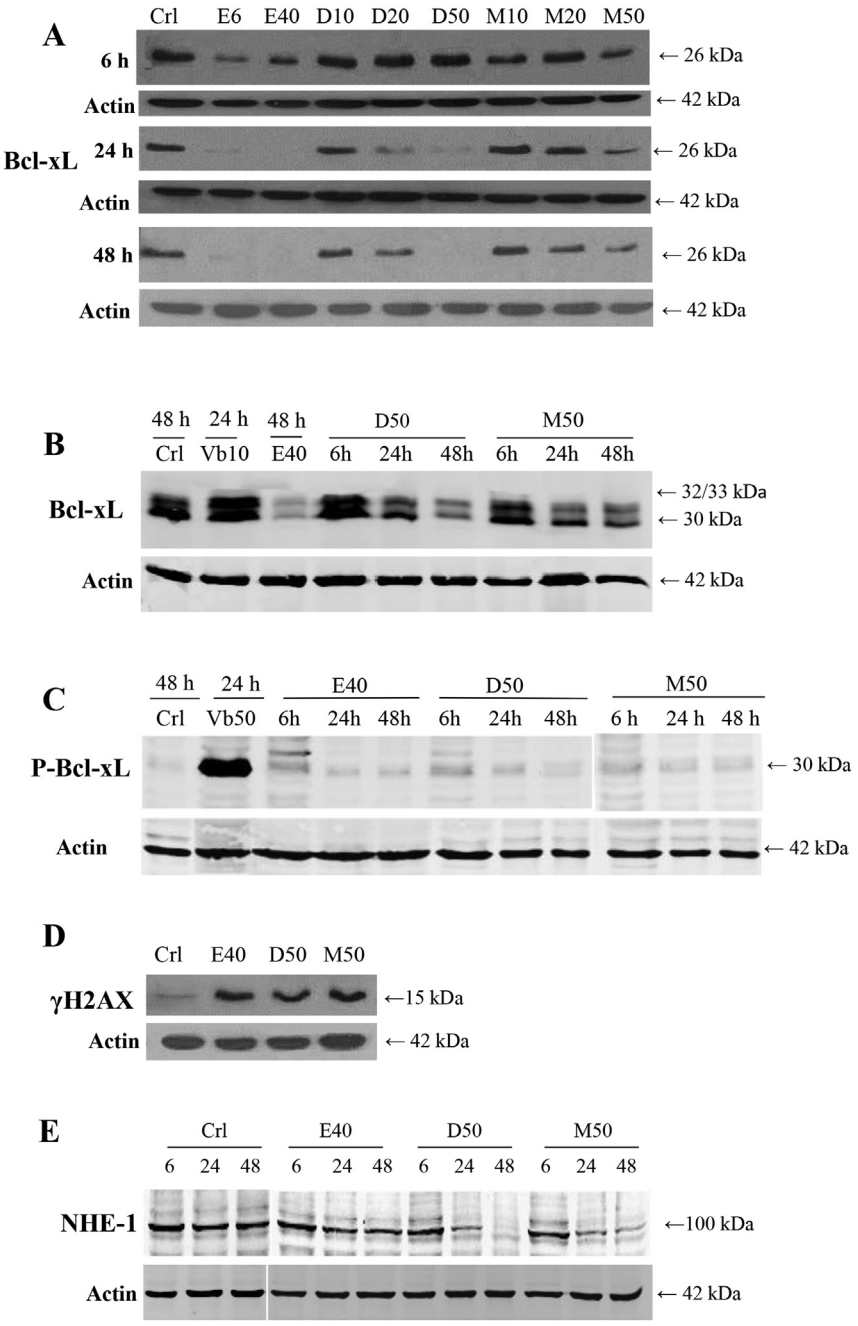

Fig. 3. *The effect of TCNAs on Bcl-xL and DNA.* Cells were incubated with doxy and mino (10, 20 and 50 μg/ml) for 6, 24 and 48 h. Etoposide (6 and 40 μg/ml) and vinblastine (10 or 50 μg/ml) served as positive controls for Bcl-xL deamidation and phosphorylation at serine 62, respectively. Cells incubated in complete media served as control. Proteins were detected using Western blot. (A) Bcl-xL, (B) Bcl-xL (54H6), (C) phospho-Bcl-xL pSer62, (D) γH2Ax, (E) NHE-1 antiporter.

Bcl-xL Ser-62) (Fig. 3C). No cleavage fragments of Bcl-xL were observed with any of the antibodies. Thus, the Bcl-xL molecule is modified by early deamidation followed by decreased protein levels.

Bcl-xL levels are continuously modulated by deamidation that reduces cellular activities of Bcl-xL and targets Bcl-xL for degradation [23]. DNA damage enhances Bcl-xL deamidation that is mediated by increased protein expression of the NHE-1 antiporter and intracellular alkalinization [24]. However, in myeloid cells from patients with CML expressing Bcr/Abl fusion protein, DNA damage did not induce either an increase in protein levels of the NHE-1 or increase in intracellular pH, nor Bcl-xL deamidation and apoptosis [25]. In myeloproliferative disorders, the oncogenic tyrosine kinases contributed to resistance to etoposide by suppression of Bcl-xL deamidation and the levels of Bcr/Abl protein correlated with the degree of inhibition of the Bcl-xL deamidation pathway [25].

In our study, DNA double strand breaks were detected as 15 kDa band of γH2AX at 6 h after the incubation start with doxy and mino (Fig. 3D). However, the levels of NHE-1 antiporter protein were not increased at 6 h after the incubation start, and at later time points the levels were reduced (Fig. 3E). The oxidative stress is considered to be a favorable condition for Bcl-xL deamidation by a mechanism that is not dependent on the increased NHE-1 activity [26]. However, in our study, no significant increase of the ROS levels was

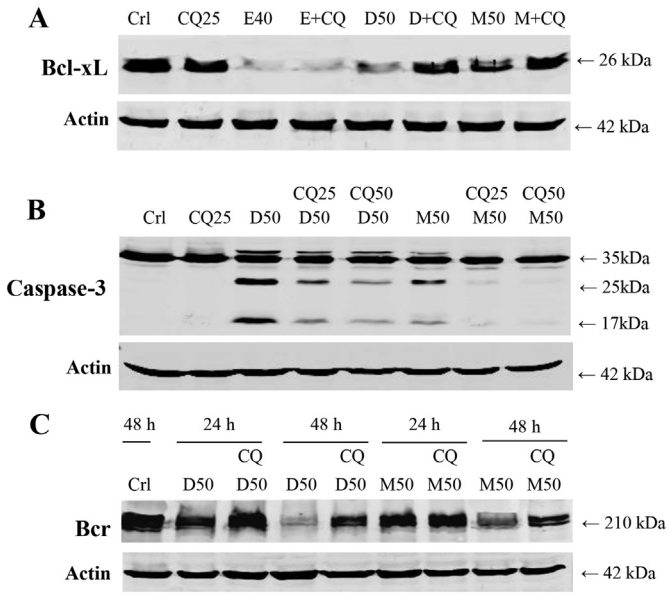

Fig. 4. *The role of lysosomal inhibitor chloroquine in TCNAs cytotoxicity.* Cells pre-incubated with CQ (25 or 50 μM) for 1 h were treated with doxy and mino (50 μg/ml) for 24 and 48 h. Etoposide (40 μg/ml) served as a positive control. Cells incubated in complete media served as a control. Protein expression was assessed using Western blot. (A) Bcl-xL, (B) caspase-3, (C) Bcr/Abl detected with antibody against Bcr.

induced by any of the drugs. On the other hand, the baseline intracellular pH in K562 cells has been reported to be significantly higher than in peripheral blood mononuclear cells and bone marrow cells [27].

Moreover, Bcr/Abl tyrosine kinase has been shown to inhibit the proapoptotic Bcl-xL deamidation pathway [25]. Thus, treatment that restores Bcl-xL deamidation pathway may overcome the Bcr/Abl resistance.

3.7. *Effect of lysosomal inhibitor chloroquine*

Co-incubation of drugs with CQ restored the Bcl-xL protein level (Fig. 4A) and inhibited caspase-3 activation (Fig. 4B). Furthermore, TCNAs treatment was associated with changes in the protein levels of the tyrosine kinases Bcr/Abl P210. A reduction in the protein levels of Bcr/Abl at 48 h after incubation start was reversed by CQ (Fig. 4C).

The lysosomal contribution to the induction of apoptosis is well established [5]. Induction of lysosomal membrane permeabilization (LMP) facilitates the release of lysosomal enzymes and protons that reduce the cytoplasmic pH, which facilitates caspase activation [28]. In the present study, we did not measure the cytoplasmic pH, but a reduction in NHE-1 antiport protein was observed (Fig. 3E). This finding may imply intracellular acidification [29]. The lysosomal pH is 4.3 ± 0.3 [28]. Doxy and mino have dissociation constants (pKa) of 3.5, 7.7 and 9.5 and 2.8, 5.0, 7.8 and 9.3, respectively [26]. The isoelectric point is 5.0 for doxy and 6.4 for mino [30,31]. Thus, lysosomes may also be considered as a cellular target for doxy and mino as has been suggested by other authors [32,33].

Conflict of interest

None.

Acknowledgments

This study was supported by grants from the Swedish Childhood Cancer Foundation (Barncancerfonden: PROJ04/085, PROJ04/098, PROJ06/121; http://www.barncancerfonden.se) and The Cancer Foundation (Cancerfonden: CAN2008/754, CAN2011/786, CAN2011/595; http://www.cancerfonden.se).

Appendix A. Supplementary data

Supplementary data related to this article can be found at http://dx.doi.org/10.1016/j.bbrc.2015.05.043.

Transparency document

Transparency document related to this article can be found online at http://dx.doi.org/10.1016/j.bbrc.2015.05.043.

References

[1] M. Rebucci, C. Michiels, Molecular aspects of cancer cell resistance to chemotherapy, Biochem. Pharmacol. 85 (2013) 1219–1226.
[2] L. Galluzzi, I. Vitale, J.M. Abrams, et al., Molecular definitions of cell death subroutines: recommendations of the Nomenclature Committee on Cell Death 2012, Cell Death Differ. 19 (2012) 107–120.
[3] C. Wang, R.J. Youle, The role of mitochondria in apoptosis*, Annu Rev. Genet. 43 (2009) 95–118.
[4] M. Feoktistova, M. Leverkus, Programmed necrosis and necroptosis signalling, FEBS J. 282 (2014) 19–31.
[5] U. Repnik, V. Stoka, V. Turk, et al., Lysosomes and lysosomal cathepsins in cell death, Biochim. Biophys. Acta 1824 (2012) 22–33.
[6] T. Onoda, T. Ono, D.K. Dhar, et al., Tetracycline analogues (doxycycline and COL-3) induce caspase-dependent and -independent apoptosis in human colon cancer cells, Int. J. Cancer. J. Int. Du Cancer 118 (2006) 1309–1315.
[7] K. Son, S. Fujioka, T. Iida, et al., Doxycycline induces apoptosis in PANC-1 pancreatic cancer cells, Anticancer Res. 29 (2009) 3995–4003.
[8] M.H. Pourgholami, A.H. Mekkawy, S. Badar, et al., Minocycline inhibits growth of epithelial ovarian cancer, Gynecol. Oncol. 125 (2012) 433–440.
[9] A. Bedi, J.P. Barber, G.C. Bedi, et al., BCR-ABL-mediated inhibition of apoptosis with delay of G2/M transition after DNA damage: a mechanism of resistance to multiple anticancer agents, Blood 86 (1995) 1148–1158.
[10] S. Ray, G. Bullock, G. Nunez, et al., Enforced expression of Bcl-XS induces differentiation and sensitizes chronic myelogenous leukemia-blast crisis K562 cells to 1-beta-D-arabinofuranosylcytosine-mediated differentiation and apoptosis, Cell Growth Differ. 7 (1996) 1617–1623.
[11] T. Onoda, T. Ono, D.K. Dhar, et al., Doxycycline inhibits cell proliferation and invasive potential: combination therapy with cyclooxygenase-2 inhibitor in human colorectal cancer cells, J. Laboratory Clin. Med. 143 (2004) 207–216.
[12] Z.A. Sekeroglu, F. Afan, V. Sekeroglu, Genotoxic and cytotoxic effects of doxycycline in cultured human peripheral blood lymphocytes, Drug Chem. Toxicol. 35 (2012) 334–340.
[13] M. Tolomeo, S. Grimaudo, S. Milano, et al., Effects of chemically modified tetracyclines (CMTs) in sensitive, multidrug resistant and apoptosis resistant leukaemia cell lines, Br. J. Pharmacol. 133 (2001) 306–314.
[14] Y. Guo, S.M. Srinivasula, A. Druilhe, et al., Caspase-2 induces apoptosis by releasing proapoptotic proteins from mitochondria, J. Biol. Chem. 277 (2002) 13430–13437.
[15] V. Prasad, A. Chandele, J.C. Jagtap, et al., ROS-triggered caspase 2 activation and feedback amplification loop in beta-carotene-induced apoptosis, Free Radic. Biol. Med. 41 (2006) 431–442.
[16] C. Maas, E. de Vries, S.W. Tait, et al., Bid can mediate a pro-apoptotic response to etoposide and ionizing radiation without cleavage in its unstructured loop and in the absence of p53, Oncogene 30 (2011) 3636–3647.
[17] M. Zoratti, I. Szabo, U. De Marchi, Mitochondrial permeability transitions: how many doors to the house? Biochim. Biophys. Acta 1706 (2005) 40–52.
[18] R. Kumarswamy, S. Chandna, Putative partners in bax mediated cytochrome-c release: ANT, CypD, VDAC or none of them? Mitochondrion 9 (2009) 1–8.
[19] J.E. Kokoszka, K.G. Waymire, S.E. Levy, et al., The ADP/ATP translocator is not essential for the mitochondrial permeability transition pore, Nature 427 (2004) 461–465.
[20] S. Shimizu, M. Narita, Y. Tsujimoto, Bcl-2 family proteins regulate the release of apoptogenic cytochrome c by the mitochondrial channel VDAC, Nature 399 (1999) 483–487.
[21] M. Upreti, E.N. Galitovskaya, R. Chu, et al., Identification of the major phosphorylation site in Bcl-xL induced by microtubule inhibitors and analysis of its functional significance, J. Biol. Chem. 283 (2008) 35517–35525.
[22] B.E. Deverman, B.L. Cook, S.R. Manson, et al., Bcl-xL deamidation is a critical switch in the regulation of the response to DNA damage, Cell 111 (2002) 51–62.
[23] S.H. Dho, B.E. Deverman, C. Lapid, et al., Control of cellular Bcl-xL levels by deamidation-regulated degradation, PLoS Biol. 11 (2013) e1001588.
[24] R. Zhao, D. Oxley, T.S. Smith, et al., DNA damage-induced Bcl-xL deamidation is mediated by NHE-1 antiport regulated intracellular pH, PLoS Biol. 5 (2007) e1.

[25] R. Zhao, G.A. Follows, P.A. Beer, et al., Inhibition of the Bcl-xL deamidation pathway in myeloproliferative disorders, N. Engl. J. Med. 359 (2008) 2778–2789.
[26] A. Cimmino, R. Capasso, F. Muller, et al., Protein isoaspartate methyltransferase prevents apoptosis induced by oxidative stress in endothelial cells: role of Bcl-Xl deamidation and methylation, PloS One 3 (2008) e3258.
[27] I.N. Rich, D. Worthington-White, O.A. Garden, et al., Apoptosis of leukemic cells accompanies reduction in intracellular pH after targeted inhibition of the Na(+)/H(+) exchanger, Blood 95 (2000) 1427–1434.
[28] C. Nilsson, U. Johansson, A.C. Johansson, et al., Cytosolic acidification and lysosomal alkalinization during TNF-alpha induced apoptosis in U937 cells, Apoptosis Int. J. Program. Cell Death 11 (2006) 1149–1159.
[29] S. Akram, H.F. Teong, L. Fliegel, et al., Reactive oxygen species-mediated regulation of the Na+-H+ exchanger 1 gene expression connects intracellular redox status with cells' sensitivity to death triggers, Cell Death Differ. 13 (2006) 628–641.
[30] S. Shariati, Y. Yamini, A. Esrafili, Carrier mediated hollow fiber liquid phase microextraction combined with HPLC-UV for preconcentration and determination of some tetracycline antibiotics, J. Chromatogr. B Anal. Technol. Biomed. Life Sci. 877 (2009) 393–400.
[31] A.G. Butterfield, D.W. Hughes, N.J. Pound, et al., Separation and detection of tetracyclines by high-speed liquid chromatography, Antimicrob. Agents Chemother. 4 (1973) 11–15.
[32] Y. Gu, N. Singh, Doxycycline and protein folding agents rescue the abnormal phenotype of familial CJD H187R in a cell model, Brain Res. Mol. brain Res. 123 (2004) 37–44.
[33] R.S. Kalish, S. Koujak, Minocycline inhibits antigen processing for presentation to human T cells: additive inhibition with chloroquine at therapeutic concentrations, Clin. Immunol. 113 (2004) 270–277.